THE ASTROPHYSICAL JOURNAL, 409:170–178, 1993 May 20

MOLECULAR GAS IN POWERFUL RADIO GALAXIES DETECTED BY *IRAS*

J. M. MAZZARELLA,[1,2] J. R. GRAHAM,[2,3] D. B. SANDERS,[4] AND S. DJORGOVSKI[5,6]

Received 1992 September 23; accepted 1992 November 16

ABSTRACT

Results are presented from the first phase of a CO($J = 1 \rightarrow 0$) line survey of powerful radio galaxies (log $P_{408\,\mathrm{MHz}} \gtrsim 23.5$ W Hz^{-1}). Eight radio galaxies detected by *IRAS* have been observed to a sensitivity limit of $\sim$1.0 mK rms (45 km s^{-1} resolution) using the new 3 mm SIS receiver on the NRAO 12 m telescope; five sources were detected. These observations include the CO detection of the highly variable, compact flat-spectrum radio galaxy 3C 120, detections of four galaxies from the Bologna B2 radio sample, and establishment of sensitive upper limits on the molecular gas content of the very powerful radio galaxies 4C 29.30, 3C 321, and Cygnus A (3C 405). These data have doubled the number of CO detections of powerful radio galaxies, allowing us to begin exploration of the full range of CO luminosities characteristic of this class of objects. The range of computed molecular gas masses, log $M(\mathrm{H_2})/M_\odot = 9.42 - 10.34$, is $\sim$1–7 times the H_2 mass of the Milky Way and is in stark contrast to the low molecular gas masses found in radio-quiet far-infrared–selected elliptical galaxies, log $M(\mathrm{H_2})/M_\odot \sim 7$–8. The relatively high CO detection rate for the current sample suggests that rich supplies of molecular gas may be ubiquitous in powerful radio-selected galaxies detected by *IRAS*. The infrared luminosity to molecular gas mass ratio, $L_{ir}/M(\mathrm{H_2})$, in powerful radio galaxies observed in CO is in the range $\sim 15\ L_\odot\ M_\odot^{-1}$ to $> 100\ L_\odot\ M_\odot^{-1}$, typical of the range of values found in infrared-luminous nuclear starbursts and AGNs. The CO($J = 1 \rightarrow 0$) line widths of 3C 120, B2 0722+300, and B2 1318+343 are very broad (FWZI $\gtrsim 500$ km s^{-1}) compared to normal galaxies, but consistent with previously observed interacting/merging galaxies. The CO profile for B2 1506+345 is bimodal; both components of this galaxy pair each contain $\sim 10^{10}\ M_\odot$ of molecular gas. The new CO observations support the hypothesis that powerful radio galaxies originate in colliding disk galaxies which evolve into gas-rich, peculiar E/S0 galaxies during the merger process.

Subject headings: galaxies: ISM — infrared: galaxies — ISM: molecules — radio continuum: galaxies

1. INTRODUCTION

One of the many exciting discoveries made by *IRAS* is that a significant fraction of radio galaxies are luminous far-infrared (FIR) sources (Golombek, Miley, & Neugebauer 1988). Since the *IRAS* data provide a sensitive indicator for the presence of a large amount of interstellar material, this discovery has motivated the study of the cold atomic (H I) and molecular (CO) gas components in radio galaxies. Current published CO data on radio galaxies is limited to a small number of objects that were studied as part of infrared selected galaxy samples. Nevertheless, recent observations of CO and H I have shown that cold gas is an important constituent of some powerful radio galaxies (Mirabel 1989; Mirabel, Sanders, & Kazes 1989), although the number of such objects observed to date is very small. Optical imaging of powerful radio galaxies shows evidence for morphological peculiarities which take the form of tails and bridges typical of spiral galaxies undergoing tidal interaction, suggesting that they probably arise from the collision or merger of galaxy pairs, at least one member of which is a disk galaxy (Heckman et al. 1986). Likewise, Sanders et al. (1988a, b) have proposed that classical UV-excess quasars may evolve from ultraluminous infrared galaxies which apparently involve interactions and mergers of gas-rich disk galaxies. Overlap in optical morphology and molecular gas properties, combined with new evidence that large-scale radio lobes are in an early stage of development in at least one ultraluminous infrared system that clearly involves a disk/disk merger, Mrk 463 (Mazzarella et al. 1991), suggests that powerful radio galaxies, luminous infrared galaxies, and quasars may have a common origin. Such a scenario would not be surprising given increasing observational evidence that the observed differences between such objects may be due to geometric orientation and beaming effects (e.g., Barthel 1989), nuclear obscuration (e.g., Djorgovski et al. 1991), and perhaps the dynamical age of the triggering interaction.

Since an ample supply of interstellar material is presumably required to fuel the central engine responsible for the observed outflow of radio emitting plasma, the nature of the interstellar medium in radio galaxies is also of great interest. However, until recently it was commonly believed that the hosts of strong radio emitting nuclei were elliptical galaxies, and early observations indicated that elliptical galaxies are gas poor relative to spiral galaxies (e.g., Faber & Gallagher 1976). Large molecular gas masses are therefore not expected in radio galaxies. Nevertheless, more recent evidence leads us to doubt the picture of radio galaxies as gas-poor ellipticals. The hosts of powerful radio sources are now known to differ substantially from normal elliptical galaxies (e.g., Heckman et al. 1986). Nearby examples such as Centaurus A and Cygnus A show extensive optical morphological peculiarities. In addition, observations of H I absorption and CO emission (van der Hulst, Golisch, & Haschick 1983; Phillips et al. 1987) provide strong support for the picture of Cen A as an elliptical which

[1] Infrared Processing & Analysis Center, MS 100-22, California Institute of Technology, Jet Propulsion Laboratory, Pasadena, CA 91125.
[2] Division of Physics, Mathematics and Astronomy, California Institute of Technology, Pasadena, CA 91125.
[3] Department of Astronomy, University of California, Berkeley, CA 94720.
[4] Institute for Astronomy, University of Hawaii, Honolulu, HI 96822.
[5] Department of Astronomy, MS 105-24, California Institute of Technology, Pasadena, CA 91125.
[6] Presidential Young Investigator.

has "accreted" a spiral galaxy. Near-infrared imaging of Cygnus A has revealed a luminous pointlike nucleus which is apparently extinguished by $A_V \sim 50$ mag (Djorgovski et al. 1991). Perhaps the most striking anomaly is the discovery of strong CO fluxes indicating large total H_2 masses in Perseus A (= 3C 84 = NGC 1275), 3×10^9 $M_\odot$, and PKS 1345+12 (= 4C 12.50), 6×10^{10} $M_\odot$ (Mirabel et al. 1989). The host galaxies for these powerful radio sources are clearly not typical ellipticals deficient in cold interstellar gas.

To better quantify the molecular gas content of poweful radio galaxies, and to understand how their molecular gas and infrared properties compare with other types of objects, we have begun a program of CO($J = 1 \rightarrow 0$) observations of a complete sample of powerful radio galaxies. This paper presents initial results from observations of eight powerful radio galaxies with radio power log $P_{408\ \mathrm{MHz}} \gtrsim 23.5$ (W Hz^{-1}). In § 2 the sample, observations and data reduction are described; § 3 presents the observed CO profiles and derived molecular gas properties. In § 4 the properties of the radio galaxies are examined in relation to other classes of objects including normal spirals, elliptical galaxies, luminous infrared galaxies, and quasars with available CO data. Section 5 summarizes our results. Throughout this paper we have used $H_0 = 75$ km s^{-1} Mpc^{-1}.

2. SAMPLE SELECTION AND OBSERVATIONS

2.1. *Sample Selection*

The observed radio galaxies are part of an infrared flux-limited sample with 60 μm flux greater than 0.3 Jy derived from the catalog of radio galaxies of Burbidge & Crowne (1979) using the *IRAS* data of Golombek et al. (1988). The objects were chosen to fully cover the sky, and to be relatively near ($z < 0.1$), but otherwise were not subject to bias. The radio galaxies span a large range of power, (log $P_{408\ \mathrm{MHz}} \simeq 23.5$–28.5 W Hz^{-1}), radio structures (compact flat-spectrum, Fanaroff-Riley [1974] types I and II), optical spectra (weak and strong emission lines, Seyfert types 1 and 2), and FIR spectral shape, including the relatively flat (νf_ν) spectral energy distribution of 3C 120, to objects with moderate 40–120 μm "bumps," to strong FIR-excess objects like B2 1318+343.

2.2. *Observations*

The CO($J = 1 \rightarrow 0$) observations were made during the period 1991 November 5–9 at the NRAO[7] 12 m telescope (HPBW = 55″ at 115 GHz). The telescope was equipped with a new sensitive dual-polarization SIS receiver with a temperature of ~70 K (SSB) in each channel. For the majority of the observing period the weather was clear and relatively dry. Over the redshifted CO($1 \rightarrow 0$) frequency range of ~104–113 GHz the system temperature was ~150–250 K. Two 256 channel filterbanks of 2 MHz filters, one for each polarization, provided a total velocity coverage of ~1550 km s^{-1} with a resolution of ~6 km s^{-1}. The observations were made in beam-switched mode using a subreflector that nutates at a frequency of 1.25 Hz. This observing mode provided exceptionally flat baselines. Pointing was monitored by observations of planets and quasars and was estimated to be accurate to ±4″ (rms). The allotted observing time was sufficient to observe eight radio galaxies to a common sensitivity limit of ~1 mK (3 σ at 45 km s^{-1} resolution).

[7] The NRAO is operated by Associated Universities, Inc., under cooperative agreement with the National Science Foundation.

The spectra were obtained with the spectrometer passband centered on the optical or H I redshift. The majority of the sources were observed for a total period of 6–12 hr, with the data taken in two to four separate blocks of time. The longest integration was for a total time of 20 hr on Cygnus A. For each source, the center frequency was shifted slightly (typically ±50 MHz) between separate data blocks to both test the reality of weak signals and to minimize any systematic baseline ripples. The spectra were calibrated using an ambient temperature chopper wheel and scaled by the telescope efficiency on a spatially extended source, $\eta_{\mathrm{fss}} \equiv \eta_{\mathrm{moon}}$, to give line temperatures T_R^*. After co-adding both polarizations, the CO spectra were Gaussian smoothed to a resolution of 45 km s^{-1} giving a typical rms noise of 0.3–0.6 mK.

3. RESULTS

The CO data are presented in Table 1, along with new estimates of the *IRAS* flux densities for the observed galaxies. The eight sources observed in the CO($J = 1 \rightarrow 0$) line are listed by their best known radio catalog names, with aliases listed here: 3C 120 (= UGC 03087 = Mrk 1506 = II Zw 014), B2 0648+275 (= Zw 145.017), B2 0722+300 (= Zw 147.020), 4C 29.30 (= Zw 150.014 = B2 0836+29B), B2 1318+343 (= IC 883 = UGC 08387 = I Zw 056 = Arp 193 = VV 821), B2 1506+345 (= Zw 193.016 = VV 059), 3C 321 (= 4C 24.34 = B2 1529+242), and Cygnus A (= 3C 405 = 4C 40.40 = VV 072). The radio positions listed in the table correspond to the observed coordinates at the 12 m telescope. The *IRAS* fluxes were determined from either ADDSCAN data or, when available, from pointed observations. Due to improvements in processing the *IRAS* data, the fluxes are slightly different than those previously published by Golombek, Miley, & Neugebauer (1988). Figure 1 presents the CO spectra.

The CO observations produced four strong detections, one weak detection, and three upper limits. The CO line parameters listed in Table 1 where determined from the final spectra shown in Figure 1. The redshift, z ($\equiv \Delta\lambda/\lambda$), and velocity line widths (ΔV_{50}, ΔV_{00}) correspond to the mean velocity of the CO emission profile, and the FWHM and FWZI, respectively. For the three nondetections the velocity corresponding to the center of the filterbank has been given in parentheses. The peak temperature is in units of T_R^* and can be converted to flux by multiplying by the system sensitivity of the 12 m telescope (31 Jy K^{-1}). The final column in Table 1 gives the integrated CO emission line intensity. The upper limits on the CO integrated intensity for the three nondetections are discussed below.

Table 2 gives infrared luminosities, dust temperatures, dust masses, and H_2 masses derived from the data in Table 1. The distances for each object listed in Table 2 were calculated from the redshifts using the Virgocentric flow model of Aaronson et al. (1982), assuming $H_0 = 75$ km s^{-1} Mpc^{-1} and $q_0 = 0$. Table 2 also lists visual and radio data from Golombek, Miley, & Neugebauer (1988). The infrared luminosities were computed using the procedure outlined by M. Pérault & F. Boulanger (1986, unpublished), employing data from all four *IRAS* bands to approximate an infrared luminosity, L_{ir}, from 8 to 1000 μm. This method provides a significantly better determination of the total FIR/submillimeter luminosity than the more commonly used L_{fir}, determined by fitting a single-temperature dust model of the 60 and 100 μm fluxes (cf. Cataloged Galaxies and Quasars Detected in the *IRAS* Survey 1985). L_{fir} is also given in Table 2. The ratio of 60 and 100 μm fluxes was also

TABLE 1

CO($J = 1 \rightarrow 0$) AND *IRAS* OBSERVATIONS OF RADIO GALAXIES

Name	R.A. 1950	Decl. 1950	Flux Densities, S_ν: 12 μm (Jy)	25 μm (Jy)	60 μm (Jy)	100 μm (Jy)	cz (km s^{-1})	CO Line Parameters: ΔV_{50} (km s^{-1})	ΔV_{00} (km s^{-1})	T_P (mK)	$\int T_R^* dV$ (K km s^{-1})
3C 120	4ʰ30ᵐ31ˢ.6	5°15′00″	0.30	0.67	1.34	2.97	9920	500	710	2.3	1.15
B2 0648+275	6 48 54.2	27 31 17	0.14	0.96	2.44	1.76	12420	220	250	1.5	0.30
B2 0722+300	7 22 27.8	30 3 20	0.20	0.41	3.02	4.33	5650	480	520	4.1	1.55
4C 29.30	8 36 59.0	29 59 44	<0.10	0.13	0.50	0.45	(19270)	...	...	<2.2[a]	...
B2 1318+343	13 18 16.9	34 23 56	0.26	1.39	15.91	24.37	6990	400	520	19.1	7.10
B2 1506+345	15 6 5.6	34 34 18	0.15	0.22	2.64	5.63	13467	...	725	...	1.86
Component 1							13300	195	380	4.7	0.96
Component 2							13660	225	400	4.3	0.90
3C 321	15 29 33.5	24 14 27	<0.07	0.30	1.07	1.17	(29050)	...	...	<2.2	...
Cygnus A (3C 405)	19 57 44.4	40 35 45	0.21	0.87	2.47	<2.5	(17300)	...	...	<1.3	...

[a] 3 times the channel-to-channel rms.

used to estimate the mass of "warm dust" detected by *IRAS*. A single-temperature dust model was fitted to the 60 and 100 μm *IRAS* fluxes using dust emissivities from Draine & Lee (1984). For the dust temperatures and FIR luminosities listed in Table 2, $M_{\rm dust} = (L_{\rm fir}/10^8\,L_\odot)(40\,{\rm K}/T_{\rm dust})^5\,10^4\,M_\odot$.

The total mass of molecular gas, $M(H_2)$, has been computed from the integrated CO intensity assuming a constant conversion factor between the CO line emission and the molecular hydrogen mass: $M(H_2)\,(M_\odot) = 4.78 L_{\rm CO}$ (K km s^{-1} pc^2) (see Appendix A of Sanders, Scoville, & Soifer 1991). The constant 4.78 corresponds to a CO to H_2 conversion factor of $\alpha = 3 \times 10^{20}$ cm^{-2} (K km s^{-1})$^{-1}$. It represents a mean of the determinations in the literature based on virial mass estimates for Galactic clouds (see Scoville & Sanders 1987), and observations of Galactic γ-rays (Bloemen et al. 1986). As in previous analyses of extragalactic CO data, we have implicitly assumed that the molecular cloud properties in the radio galaxies, specifically the density and temperature, are similar to those for molecular clouds in the Milky Way. The use of a similar conversion factor is also justified given that $M(H_2)/L_{\rm CO} \propto \rho^{1/2} T^{-1}$ (Dickman, Snell, & Schloerb 1986; Scoville & Sanders 1987), so the density and temperature of the molecular gas may offset each other in the high-luminosity radio galaxies where both the density and temperature are probably higher than in our Galaxy.

For those objects not detected in CO, a conservative estimate for the upper limit on the CO integrated intensity and the corresponding H_2 mass was made by assuming a Gaussian line with FWHM similar to the mean line width for the detected galaxies and a line peak temperature equal to 3 times the rms determined for the spectrum.

4. DISCUSSION

4.1. *Individual Source Descriptions*

3C 120 (= UGC 03087 = Mrk 1506 = II Zw 014). Optically, this object appears as an isolated, peculiar S0 galaxy ~40″ (25 kpc) in diameter with a luminous Seyfert 1/quasar nucleus, a jetlike feature extending 12″ (8 kpc) from the center at P.A. = 315°, and a bright extended emission-line nebula in the light of Hα + [N II] and [O III] λ5007 (Balick & Heckman 1979; Heckman et al. 1986; Moles et al. 1988). It is not clear whether the peculiar optical morphology, perturbed rotation curve and wide-spread enhanced star formation are due to the effects of tidal perturbation or interaction of the radio jet with the galaxy. However, Heckman et al. (1986) and Moles et al. (1988) have suggested that the data are consistent with a merger that is near completion. This remarkable object has been the subject of extensive radio imaging studies. It has a highly variable flat-spectrum radio core, a one-sided curved jet extending approximately westward with superluminal motion, and a complex radio morphology extending over the vast scale of ~500 kpc (Walker et al. 1987). The new CO data add substantial support to the hypothesis that 3C 120 involves a merger of gas-rich galaxies. The CO($J = 1 \rightarrow 0$) line profile is

TABLE 2

IR/RADIO LUMINOSITIES AND H_2 MASSES OF RADIO GALAXIES

Name	D (Mpc)	Optical Emission	M_V (mag)	Radio Class	log P_{408} (W Hz^{-1})	T_D (K)	M_D ($M_\odot$)	log $L_{\rm fir}$ ($L_\odot$)	log $L_{\rm ir}$ ($L_\odot$)	log $M(H_2)$ ($M_\odot$)	$L_{\rm ir}/M(H_2)$ ($L_\odot/M_\odot$)
3C 120	130.4	SE/S1	−22.0	FC	25.02	41	6.68	10.72	11.10	9.79	20
B2 0648+275	166.4	WE	−21.4	Compact	23.95	68	6.13	11.29	11.37	9.42	89
B2 0722+300	77.0	SE	−19.0	F-R I	23.43	38	6.72	10.63	10.77	9.47	20
4C 29.30	258.9	SE	−21.6	F-R I	25.12	43	6.70	10.84	11.13	<9.51	>43
B2 1318+343	98.4	WE	−20.3	Compact	25.36	37	7.71	11.52	11.60	10.34	18
B2 1506+345	184.8	WE	−20.9	Compact	24.01	40	7.34	11.32	11.45	10.31	14
Component 1										10.01	...
Component 2										10.00	...
3C 321	392.1	SE	−22.3	F-R II	26.20	51	7.06	11.58	11.80	<9.87	>87
Cygnus A	234.5	SE/S2	−20.5	F-R II	28.44	64	6.57	11.59	11.71	<9.54	>147

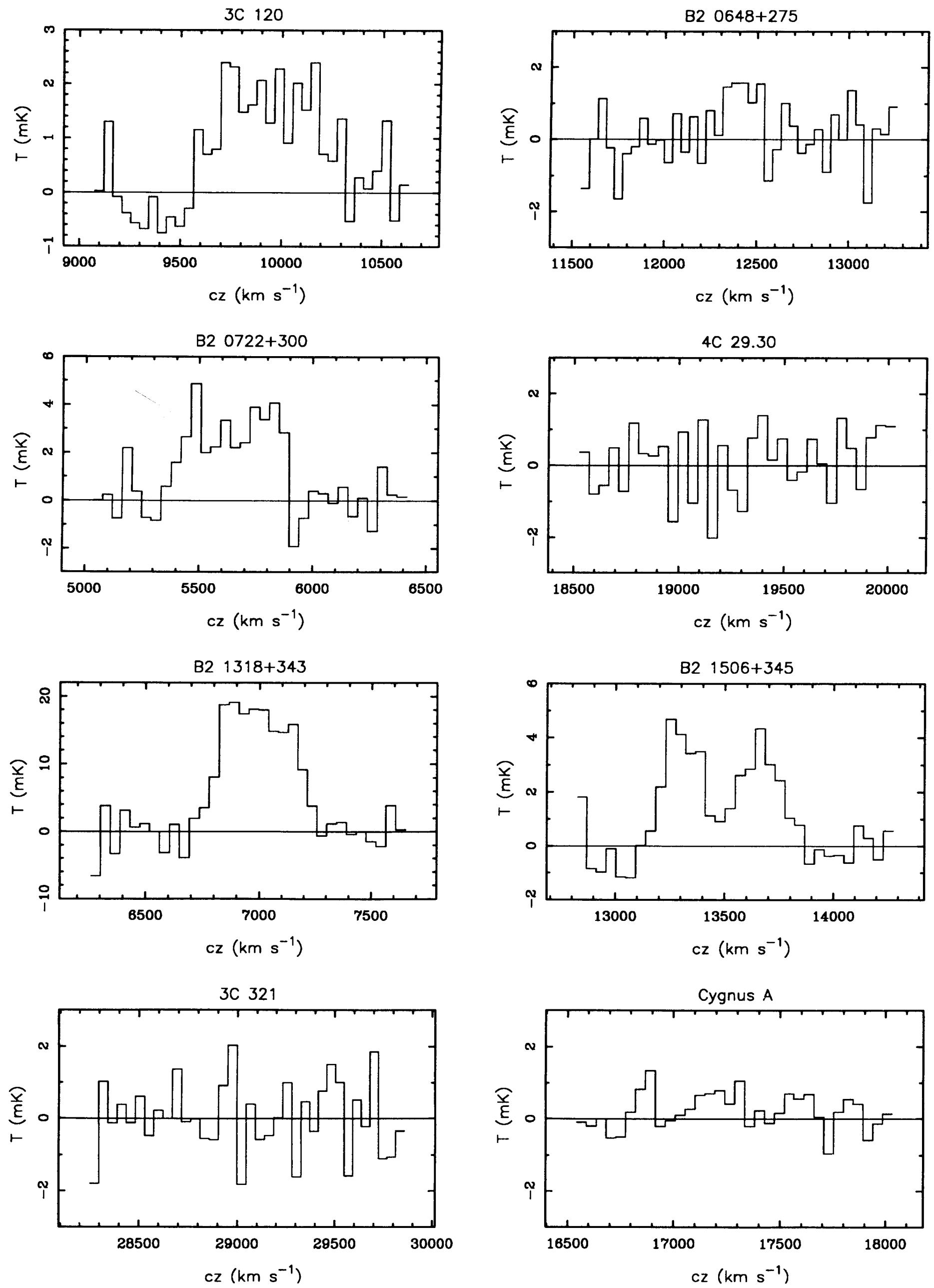

FIG. 1.—New CO($J = 1 \rightarrow 0$) observations of powerful radio galaxies detected by *IRAS*. The CO spectra were Gaussian smoothed to a resolution of 45 km s^{-1} giving a typical rms noise of 0.3–0.6 mK.

extremely broad (FWHM = 500 km s^{-1}, FWZI = 710 km s^{-1}), with approximately the same velocity width as the entire profile of the galaxy pair B2 1506+345 (see below). For comparison, gas-rich infrared luminous galaxies in the *IRAS* Bright Galaxy Sample generally have CO($J = 1 \rightarrow 0$) line widths in the range 110–300 km s^{-1} FWHM, and the largest line widths of 480–660 km s^{-1} FWZI are associated with the mergers NGC 5256 (= Mrk 266), NGC 7592 (= Mrk 928), and Arp 220 (e.g., Sanders, Scoville, & Soifer 1991).

B2 0648+275 (= Zw 145.017). On the Palomar Observatory Sky Survey (hereafter, POSS) prints, this galaxy appears to be a peculiar elliptical or S0 galaxy with a major axis of ~30″ (24 kpc) (Colla et al. 1975). Unfortunately, there is no published deep optical continuum image for this object. However, recent narrow-band imaging in Hα + [N II] shows emission extending over ~4 kpc (Morganti, Ulrich, & Tadhunter 1992). Radio continuum maps show a compact, slightly resolved core 0.4 × 0.2 kpc in size (Parma et al. 1986). Although only weakly detected, the CO data indicate this galaxy has ~10^{10} $M_\odot$ of molecular gas. This result warrants further follow-up observations of this galaxy, particularly deeper optical and radio continuum imaging.

B2 0722+300 (= Zw 147.020). This galaxy is classified as an S0 galaxy from its appearance on the POSS (Colla et al. 1975); no deep CCD images are published for this object. This is a Fanaroff-Riley (F-R) type I radio galaxy, with a ~30″ (9 kpc) two-sided jet structure at P.A. ~ 95° and a luminous Hα + [N II] emission feature of similar size as the radio structure but at P.A. ≈ 135° (Morganti et al. 1992). As argued above for 3C 120, based on comparison with the line widths of infrared luminous galaxies that are known interacting systems (Sanders et al. 1991), the new CO data suggest that B2 0722+300 is an interacting/merging pair of gas-rich galaxies. The CO($J = 1 \rightarrow 0$) line widths (FWHM = 480 km s^{-1}, FWZI = 520 km s^{-1}) are similar to the merger B2 1318+343 (Arp 193) discussed below. Deep optical and near infrared continuum images are needed for this galaxy.

4C 29.30 (= Zw 150.014 = B2 0836+29). Based on the POSS plates, this object has been described as a close pair of elliptical galaxies in a common halo, or a "dumbbell" galaxy, with components separated by 4″, or 5 kpc (Parma et al. 1991). Deeper optical imaging reveals faint shell-like structures ~20–30″ (25–36 kpc) to the east and west of what appears to be a peculiar S0 galaxy with a compact secondary component 4″ (5 kpc) to the east of the primary nucleus (Heckman et al. 1986). The galaxy has Hα + [N II] emission extended over ~45 kpc at P.A. = 0° (Morganti et al. 1992), roughly in alignment with the radio axis but normal to the faint optical shell-like features. This is an F-R type II radio galaxy with edge-brightened lobes extending ~64″ (80 kpc) at P.A. = 20° (Parma et al. 1986). Atomic hydrogen has been detected in absorption in 4C 29.30 (Mirabel 1990). Our CO observations resulted in no CO line detection, corresponding to an upper limit of log $M(H_2)/M_\odot \lesssim 9.5$.

B2 1318+343 (= IC 883 = UGC 08387 = I Zw 056 = Arp 193 = VV 821). This is a morphologically peculiar infrared-luminous galaxy in the *IRAS* Bright Galaxy Sample (Soifer et al. 1989) which clearly involves an interaction or merger between disk galaxies. Optical imaging shows a long, nearly straight tidal tail to the SE and a fainter tail to the SW (Arp 1966). Near-infrared imaging at 2.2 μm shows a single nucleus (Bushouse & Stanford 1992), suggesting that this is an advanced merger in which the component galaxies have coalesced. This galaxy was observed previously in CO by Sanders et al. (1991); the general shape of the new spectrum is consistent with their data, but our more accurate flux is larger by a factor of ≈2.5 because Sanders et al. used an *IRAS* coordinate which is displaced ≈30″ from the more precise radio coordinate used for the current observations. Mapping in CO($2 \rightarrow 1$) and CO($1 \rightarrow 0$) shows that the molecular gas is concentrated near the nucleus (Radford, Solomon, & Downes 1991). Radio images show a compact core that is only slightly resolved, with a faint spur of emission extending a few arcseconds to the NE (Parma et al. 1986; Condon et al. 1990). The broad CO($J = 1 \rightarrow 0$) line indicated in the current data support the merger interpretation.

B2 1506+345 (= Zw 193.016 = VV 059). The POSS plates indicate that this is an interacting galaxy pair separated by ~24″ (21 kpc) (Vorontsov-Velyaminov 1959); there is no published optical or near-infrared array imaging for this object. Radio continuum images show a slightly resolved (0.7 × 0.5 kpc), core-dominated source apparently associated with the northeastern member of the galaxy pair (Parma et al. 1986; Condon & Broderick 1991). The CO($J = 1 \rightarrow 0$) line profile is clearly double, revealing that both components of this interacting pair each contain ~10^{10} $M_\odot$ of molecular gas. Clearly more detailed observations at all wavelengths are warranted for this galaxy.

3C 321 (= 4C 24.34 = B2 1529+242).—This is a very powerful F-R II radio source ~300″ (570 kpc) in total extent; the inner portions of the NW jet coincides roughly with an emission-line nebula ~15″ (29 kpc) in extent and in approximate alignment with the radio axis (Baum et al. 1988). Optical continuum imaging shows a giant peculiar elliptical with a major axis of ~40″ (75 kpc), tidal debris to the SW and two nuclei separated by ~3″ (6 kpc) (Heckman et al. 1986; Baum et al. 1988). Atomic hydrogen has been detected in absorption in this galaxy (Mirabel 1990). Our CO observations resulted in no detection, indicating an upper limit of log $M(H_2)/M_\odot \lesssim 9.9$.

Cygnus A (= 3C 405 = 4C 40.40 = VV 072). This is the nearest of the classical, very powerful double-lobed radio galaxies of the F-R II class. As discussed in § 1, there is an extensive body of evidence suggesting that Cygnus A is the result of a galaxy merger. Although 20 hr of integration on the NRAO 12 m telescope with the new SIS receivers did not result in a reliable CO line detection, these observations provide a more sensitive upper limit, log $M(H_2)/M_\odot \lesssim 9.5$, than was possible with earlier observations by Mirabel et al. (1989). We note that the CO spectrum of Cygnus A, compared to the other nondetections, does not look like random noise. The possibility that this is a ~2 σ detection of a very broad CO profile with $T_p \approx 0.5$ mK will require more sensitive observations. As discussed in more detail below, because of its relatively large distance, this upper limit does not rule out a molecular gas mass in Cygnus A that is comparable to the masses found in lower redshift radio galaxies detected in CO.

4.2. *Luminosities and* H_2 *Masses*

The H_2 masses listed in Table 2 show that the radio galaxies detected in CO are rich in molecular gas, having total molecular gas masses ~1–7 times the molecular gas content of the Milky Way, $M(H_2) \approx 3 \times 10^9$ $M_\odot$. They are in stark contrast to the low H_2 gas masses, 10^7–10^8 $M_\odot$, found in radio-quiet FIR selected ellipticals (Lees et al. 1990). The copious amounts of molecular gas in these radio galaxies indicate they have a rich ISM, consistent with the large dust masses derived from their high FIR luminosities (c.f. Table 2). It is important to note that the upper limits on $M(H_2)$ for the very powerful radio galaxies Cygnus A, 3C 321, and 4C 29.30 still allow these galaxies to have a molecular gas mass comparable to that of the Milky Way. The new CO data thus support arguments based on the shape of infrared, millimeter, and submillimeter spectral energy distributions which suggest that the FIR emission in nearby radio galaxies is due to the same processes as in normal gas-rich spiral disks and elliptical galaxies with bright FIR emission—thermal radiation from a dusty ISM (Impey, Wynn-Williams, & Becklin 1990; Knapp, Bies, & van Gorkom 1990; Knapp & Patten 1991).

Figure 2 shows the ratio of infrared luminosity to molecular gas mass, $L_{ir}/M(H_2)$, versus infrared luminosity, L_{ir}, for the new radio galaxy data. Also plotted in this diagram are other samples of galaxies with CO detections, including infrared-selected galaxies from the *IRAS* Bright Galaxy Sample (Sanders, Scoville, & Soifer 1991), ellipticals selected for their bright FIR emission (Lees et al. 1990), and other powerful radio galaxies and quasars with available CO detections. The $L_{ir}/M(H_2)$ ratio for the powerful radio galaxies ranges from ~$15\ L_\odot\ M_\odot^{-1}$ to $> 100\ L_\odot\ M_\odot^{-1}$. To place the properties of the ISM in powerful radio galaxies into perspective, the estimated global $L_{ir}/M(H_2)$ ratio for the Milky Way is ~$4\ L_\odot\ M_\odot^{-1}$, and ratios of $L_{ir}/M(H_2) \gtrsim 10\ L_\odot\ M_\odot^{-1}$ in the Milky Way are found only in the most active ~1% of molecular clouds, with the highest values (20–40 $L_\odot\ M_\odot^{-1}$) confined to the 1–5 pc massive starburst cores of giant molecular clouds such as W3 Main,

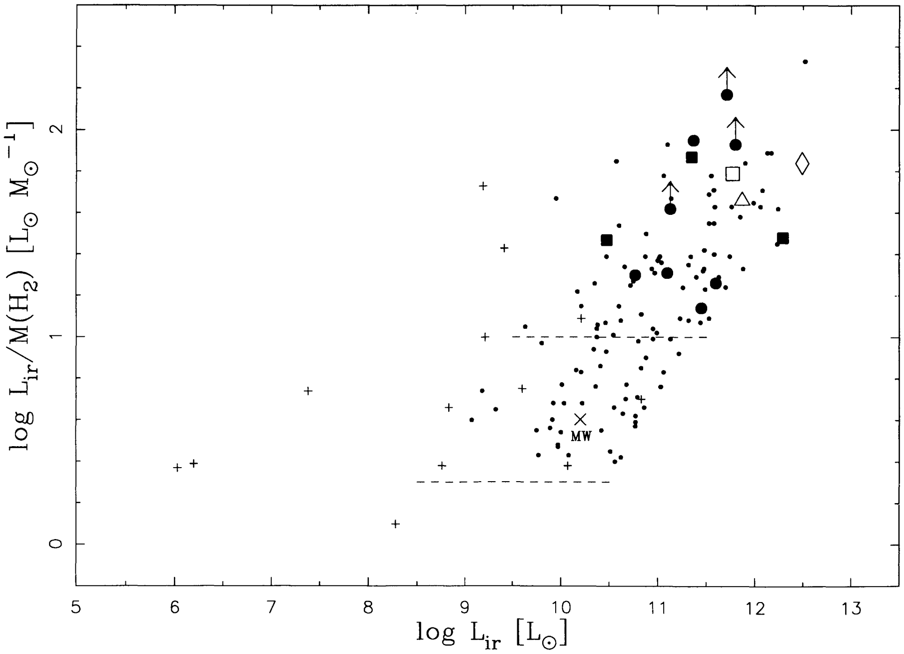

FIG. 2.—Infrared luminosity-to-molecular gas mass ratio, $L_{ir}/M(H_2)$, vs. infrared luminosity, L_{ir}. The eight radio galaxies observed in this paper (c.f., Table 2) are plotted as large solid circles, with the lower limits for Cygnus A, 3C 321, and 4C 29.30 indicated by arrows. Powerful radio-selected galaxies previously detected in CO—Perseus A, 4C 12.50 (Mirabel et al. 1989), and Centaurus A (Phillips et al. 1987)—are plotted as solid squares. Data for the infrared-warm ultraluminous galaxies Markarian 463 (Sanders et al. 1989; Mazzarella et al. 1991), Mrk 1014 (Sanders, Scoville, & Soifer 1988), and I Zw 1 (Barvainis, Alloin, & Antonucci 1989) are plotted as an open square, diamond, and triangle, respectively. The small solid circles represent infrared selected galaxies from the *IRAS* Bright Galaxy Sample (Soifer et al. 1989). The H_2 masses were derived using CO data taken from Sanders, Scoville, & Soifer (1991), Tinney et al (1990), and Young et al. (1989). Elliptical galaxies observed in CO (Lees et al. 1990) are represented as plus signs. The cross labeled "MW" indicates the global estimates of $L_{ir}/M(H_2) \sim 4$ [$L_\odot$ $M_\odot^{-1}$] and log ($L_{ir}/L_\odot$) ~ 10.2 for the Milky Way (Solomon et al. 1987; Scoville & Good 1989), and the dashed lines indicate the range $L_{ir}/M(H_2) = 2$–10 [$L_\odot$ $M_\odot^{-1}$] which is typical of the global $L_{ir}/M(H_2)$ ratios found in gas-rich spiral galaxies which are not dominated by luminous nuclear starbursts or AGNs (e.g., M51, NGC 6946, M83,—Young et al. 1986; Solomon et al. 1987; Sanders et al. 1991).

M17SW, and Sgr B2 (e.g., Solomon et al. 1987; Scoville & Good 1989). Similarly, the global $L_{ir}/M(H_2)$ ratios observed among normal molecular gas-rich spiral disks (e.g., M51, NGC 6946, M83) span a range of ~2–10 $L_\odot$ $M_\odot^{-1}$ (Young et al. 1986; Solomon et al. 1987; Sanders, Scoville, & Soifer 1991) as indicated by the dashed lines in Figure 2. In external galaxies, *global* ratios of $L_{ir}/M(H_2) \gtrsim 20$ $L_\odot$ $M_\odot^{-1}$ have been previously observed mainly in luminous infrared-selected galaxies which are often interacting/merging systems with nuclear starbursts and/or AGNs (e.g., Sanders et al. 1991). Infrared luminous galaxies with high $L_{ir}/M(H_2)$ ratios are also found to contain compact, massive nuclear concentrations of molecular gas (Scoville et al. 1991). It is tempting to conclude that the large *global* $L_{ir}/M(H_2)$ ratios derived for the powerful radio-selected galaxies observed in CO are evidence for compact massive molecular gas complexes, likely associated with nuclear starbursts and/or AGNs.

Figure 3 shows correlations between infrared luminosity and molecular gas mass with radio power for the CO galaxy samples. Unlike Figure 2, in which powerful radio galaxies fall in the same region as luminous infrared-selected galaxies, powerful radio galaxies observed in CO deviated strongly from the infrared-radio correlation for infrared selected galaxies (Fig. 3*a*). This correlation has been discussed widely in the literature and suggests an intimate link between the interstellar radiation field that heats the dust to produce the infrared emission, and the cosmic-ray particles responsible for the synchrotron radio continuum emission (e.g., Helou, Soifer, & Rowan-Robinson 1985). The weaker correlation between $M(H_2)$ and radio power (Fig. 3*b*) is a secondary relation tied to the correlation of L_{ir} with $M(H_2)$, but the radio galaxies clearly deviate from the general trend followed by infrared-selected galaxies and elliptical galaxies, just as in Figure 3*a*. There is no evidence for a significant correlation between L_{ir} or $M(H_2)$ with the 408 MHz power in observed radio galaxies. The excess radio power of these objects compared to infrared-selected galaxies with the same infrared luminosities and molecular gas masses is an indicator of the powerful radio emission from the radio cores and jets in these objects. Figure 3 reinforces the fact that our sample is indeed radio selected.

4.3. *FIR Luminous Galaxies and the Origin of Powerful Radio Galaxies*

The major result of our CO observations is the establishment of close similarities between the gross molecular gas properties [$M(H_2)$, $L_{ir}/M(H_2)$, and CO($J = 1 \rightarrow 0$) line widths] of B2 and 3CR radio galaxies and relatively radio-quiet *IRAS* Bright Galaxies with log ($L_{ir}/L_\odot$) $\gtrsim$ 10.5. The CO data therefore corroborate evidence from optical imaging that radio galaxies originate in collisions and mergers between disk galaxies (e.g., Baade & Minkowski 1954; Heckman et al. 1986). Although these CO observations strengthen the hypothesis that radio galaxies originate in collisions of galaxy disks by providing a direct detection of the gas-rich ISM in these systems, many details remain unknown. Perhaps the most basic puzzle is why are not *all* infrared luminous, gas-rich galaxies also radio-loud sources, and, likewise, why are not *all* radio galaxies also infrared luminous and rich in molecular

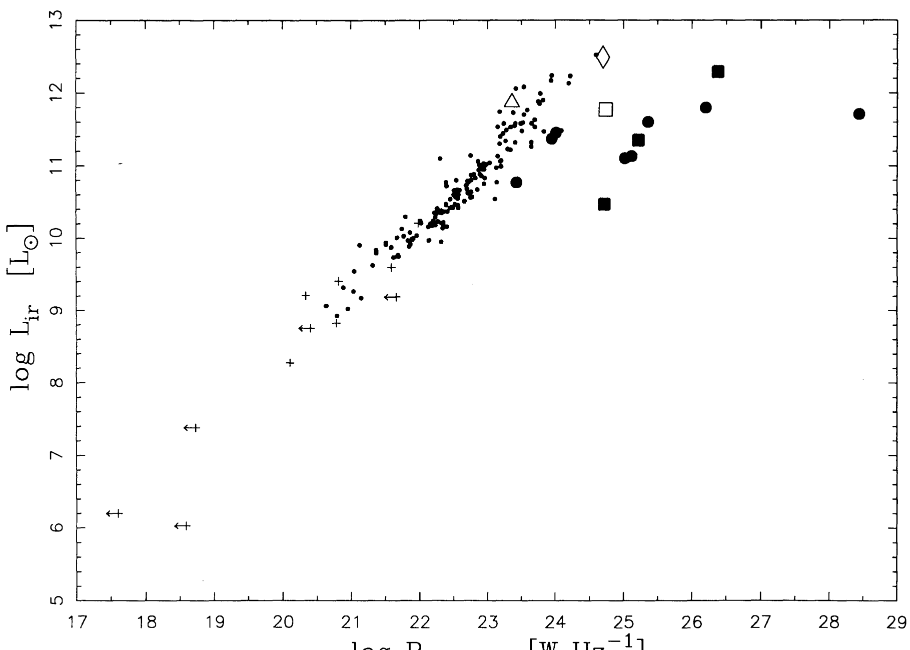

FIG. 3*a*

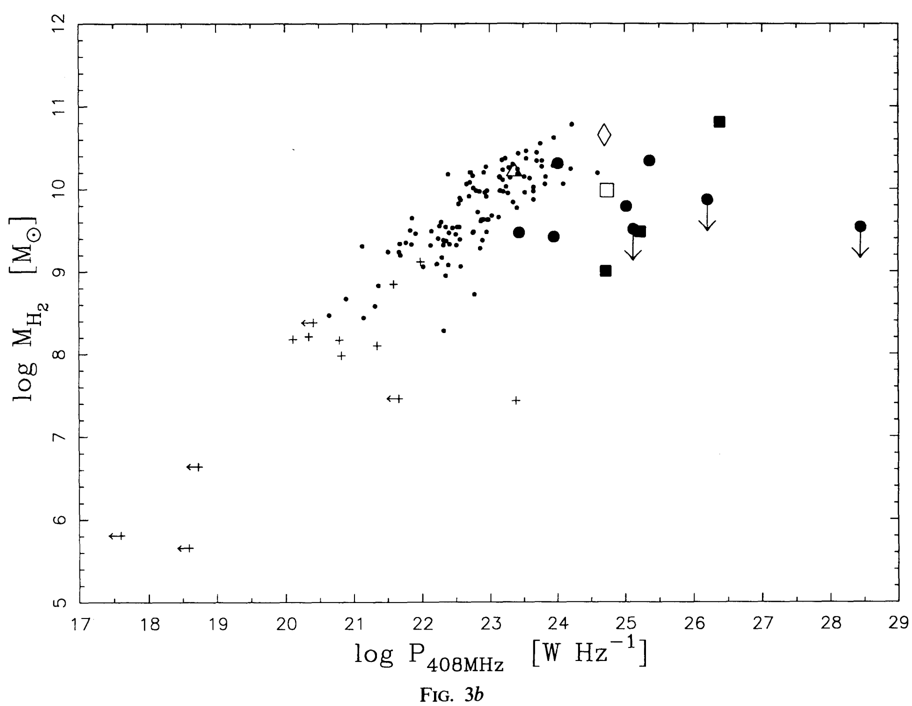

FIG. 3*b*

FIG. 3.—(*a*) Infrared luminosity, L_{ir}, vs. radio power, $P_{408 \text{ MHz}}$; (*b*) molecular gas mass, $M(H_2)$, vs. radio power, $P_{408 \text{ MHz}}$. The symbols are the same as in Fig. 2. For the UV-excess quasars Mrk 1014 and I Zw 1, $P_{408 \text{ MHz}}$ was derived from the 5000 MHz data of Kellerman et al. (1989). $P_{408 \text{ MHz}}$ for the radio galaxies are from Golombeck, Miley, & Neugebauer (1988), and $P_{408 \text{ MHz}}$ for the *IRAS* Bright Galaxies was estimated from the $P_{1499 \text{ GHz}}$ data of Condon et al. (1990), assuming a mean spectral index of -0.8 ($S_\nu \propto \nu^{-0.8}$).

gas? Another obvious question to be addressed is—is there an evolutionary progression in which radio morphology (relative dominance of core, jet, and lobes) and radio power is linked to the kinematic age of the interaction, and perhaps to other indicators of active star formation or nuclear activity?

It is tempting to conclude from the CO observations available to date that perhaps extremely powerful F-R II radio sources such as Cygnus A and 3C 321 were undetected because they are deficient in molecular gas; perhaps they have already processed much of the initial gas reservoirs supplied by the parent disk galaxies, initially into high-mass stars, and then into stellar remnants which eventually coalesced to form the supermassive central engine believed to be the ultimate source of the bright radio core and jets. In this picture, powerful F-R II sources may represent dynamically older mergers than the less powerful F-R I and compact radio sources which may originate in host galaxies which are at an earlier stage in the merger process. However, a glance at Table 2 and Figure 3 shows that it is premature to speculate about the evolution of radio galaxies based on an apparent progression of H_2 "deficiency," since the current CO upper limits for the most powerful radio sources in our sample are still consistent with molecular gas masses comparable to the H_2 mass of the Milky Way, as measured in the detected radio galaxies. More sensitive CO observations of the distant F-R II sources are needed to reach the same sensitivity in $M(H_2)$ as achieved for the closer, generally less powerful radio galaxies. It is noteworthy that two of the three radio galaxies that are currently undetected in CO, 3C 321, and 4C 29.30, have been detected in H I absorption (Mirabel 1990). Although atomic and molecular gas may both play important roles in fueling AGNs, since atomic hydrogen in absorption is commonly found in the most luminous infrared galaxies (Mirabel & Sanders 1988) which also have strong nuclear concentrations of molecular gas (Scoville et al. 1991), it is likely that 3C 321 and 4C 29.30 will be detected in CO with more sensitive measurements.

Although there are still too few classical radio galaxies with CO detections to address the questions posed above in a statistical sense, studies of related objects may provide some clues. For example, further strengthening of the connection between merging gas-rich disks and radio galaxies is provided by a particular source which, although just as luminous at radio wavelengths as the B2 radio galaxies in the current sample, was not selected in flux-limited "radio galaxy" surveys—the double-nucleus merging system Markarian 463. Based primarily on its warm FIR color temperature and its optical morphology indicating a spiral-spiral merger, Sanders et al. (1988b) included Mrk 463 in a sample proposed to represent the transition from infrared ultraluminous galaxies to classical UV-excess quasars. Recent imaging at radio and near-infrared wavelengths has shown that the eastern nucleus, Mrk 463E, has weak large-scale radio lobes with a total extent of $\sim 22''$ (22 kpc), in addition to a luminous source of 3.7 μm emission consistent with a dust-enshrouded quasar (Mazzarella et al. 1991), as suggested earlier by optical spectropolarimetry observations of an embedded broad-line region (Miller & Goodrich 1990). Given that radio sources with this spatial extent are unknown in other disk galaxies, being confined to the narrow-line regions ($\lesssim$ a few kpc) around Seyfert nuclei, it was argued that Mrk 463 represents a transition between typical Seyfert radio sources and classical radio galaxies, whereby evacuation of the ISM by starburst events triggered by a spiral-spiral merger may allow collimated radio-emitting plasma from the AGN to escape to large distances, creating radio lobes beyond the optical boundaries of the galaxy (Mazzarella et al. 1991). $CO(J = 1 \rightarrow 0)$ observations indicate Mrk 463 has an H_2 mass of 10^{10} $M_\odot$ (Sanders et al. 1989). In order to further investigate the possibility that Mrk 463 represents an important evolutionary link in the transition of a merging spiral-spiral system into a full blown powerful radio galaxy or radio-loud quasar, its position is labeled in Figures 2 and 3. The data indicate that Mrk 463 has $M(H_2)$, L_{ir}, $L_{ir}/M(H_2)$ and excess radio power similar to the B2 and 3CR radio galaxies detected in CO.

Few quasars have been observed in CO to date; detected classical UV-excess quasars include Mrk 1014 (Sanders, Scoville, & Soifer 1988) and I Zw 1 (Barvainis, Alloin, & Antonucci 1989). These sources are also "warm" *IRAS* galaxies proposed to be in a late stage in the evolution of infrared ultraluminous galaxies to classical UV-excess quasars (Sanders et al. 1988b). The presence of optical tidal features indicates that at least one of these, Mrk 1014, is the remnant of a strong tidal interaction or merger (MacKenty & Stockton 1984). The morphological evidence, and the positions of these quasars in Figures 2 and 3, add further support for a unified model which invokes a common origin for powerful radio galaxies and quasars through mergers of massive, gas-rich disk galaxies.

4.4. *Future Work*

Although the current observations have doubled the number of CO detections of powerful radio galaxies, the number of radio-selected galaxies with CO observations remains small. Clearly there is a need for additional CO observations of radio galaxies detected by *IRAS* in order to allow a search for statistical trends in the properties of radio galaxies which may depend on molecular gas properties. Observations of a larger, more complete sample are underway for this purpose. CO observations of radio galaxies which are not necessarily bright FIR sources are also needed in order to investigate the full dynamic range of molecular gas properties in extragalactic radio sources. More extensive CO observations of the nearest F-R II sources are also needed in order to reach the same sensitivity in $M(H_2)$ as achieved for the closer, less radio-powerful radio galaxies. Finally, similarities between CO and radio properties of the warm ultraluminous galaxies and the B2 and 3CR radio sources currently detected in CO suggest that a program of high dynamic range radio continuum and CO mapping of additional warm *IRAS*-selected galaxies would be valuable in order to investigate further details of the emerging evolutionary model for the genesis of powerful extragalactic radio sources.

5. SUMMARY & CONCLUSIONS

Results were presented from the first phase of a $CO(J = 1 \rightarrow 0)$ line survey of powerful radio-selected galaxies with $\log P_{408\,\mathrm{MHz}} \gtrsim 23.5$ (W Hz^{-1}). Five of eight objects observed were detected, doubling the number of reported CO detections of powerful radio galaxies. The computed H_2 masses range from $\sim 3 \times 10^9$ to $\sim 2 \times 10^{10}$ $M_\odot$, similar to the H_2 masses derived for luminous infrared galaxies, but in stark contrast to the low H_2 gas masses found in radio-quiet far-infrared selected elliptical galaxies, 10^7–10^8 $M_\odot$ (Lees et al. 1990).

The properties of B2 and 3CR powerful radio galaxies observed in CO were compared to infrared bright galaxies and elliptical galaxies with available CO data. The primary conclusions are

1. The high CO detection rate for our current sample ($\frac{5}{8}$), and the fact that the three sources not detected—Cygnus A, 3C 321, and 4C 29.30—are the most distant galaxies in the sample, with upper limits that still allow up to $\sim 3 \times 10^9$ $M_\odot$ of H_2 gas, suggests that rich supplies of molecular gas may be ubiquitous in powerful radio-selected galaxies detected by *IRAS*. The large H_2 gas masses are consistent with the hypothesis that the FIR emission from powerful radio galaxies detected by *IRAS* is thermal emission from dust.

2. The $L_{ir}/M(H_2)$ ratios for powerful radio galaxies with CO observations range from ~ 15 $L_\odot$ $M_\odot^{-1}$ to >100 $L_\odot$ $M_\odot^{-1}$, typical of the values found for luminous infrared-selected galaxies that are interacting/merging systems with nuclear starbursts and/or AGNs. Although powerful radio galaxies detected by *IRAS* and luminous infrared galaxies lie in similar regions of L_{ir} versus $M(H_2)$ and $L_{ir}/M(H_2)$ versus L_{ir} plots, the

former show their excess radio power through strong deviations from the relatively tight radio-infrared correlation for normal disk and nuclear starburst galaxies.

3. The CO($J = 1 \rightarrow 0$) line widths of 3C 120, B2 0722+300, and B2 1318+343 are extremely broad (FWZI $\gtrsim$ 500 km s^{-1}) compared to normal galaxies, but consistent with previously observed interacting/merging galaxies. The CO profile for B2 1506+345 is bimodal, indicating that both components of this interacting galaxy pair each contain $\sim 10^{10}\ M_{\odot}$ of molecular gas (H_2).

4. Comparison with the infrared and CO properties of the infrared-warm ultraluminous galaxies Mrk 463, Mrk 1014, and I Zw 1 suggests that the origin of powerful radio galaxies may be closely related to the genesis of dust-enshrouded quasars and classical UV-excess quasars through the merging of gas-rich disk galaxies (e.g., Sanders et al. 1988a, b). Furthermore, the recent detection of weak large-scale lobes associated with the compact, steep-spectrum radio core of Mrk 463E (Mazzarella et al. 1991), bolsters the case for a unified model for the origin of quasars and powerful radio galaxies.

These initial results suggest strongly that among powerful radio galaxies detected by *IRAS*, the global FIR emission is associated with a dusty ISM and a rich reservoir of molecular gas, not too unlike the conditions in infrared-luminous, interacting/merging disk galaxies in the *IRAS* Bright Galaxy Sample. Over all, the new CO observations provide support for the hypothesis that powerful radio galaxies originate from dusty, gas-rich disk galaxies which evolve into giant, peculiar E/S0 galaxies during the merger process. Although these observations have doubled the number of CO detections of powerful radio galaxies, the number of 3CR and B2 radio galaxies with CO observations remains small. Further CO observations of radio-selected galaxies are needed to address the many questions which remain concerning the evolution of powerful extragalactic radio sources.

We thank the NRAO for allocation of observing time on the 12 m telescope. An anonymous referee provided an important comment which led to an improved presentation of our results. This work was supported by the Jet Propulsion Laboratory, California Institute of Technology, under a contract with the National Aeronautics and Space Administration. This research has made use of the NASA/IPAC Extragalactic Database (NED) which is operated by the Jet Propulsion Laboratory, California Institute of Technology, under contract with the National Aeronautics and Space Administration. D. B. S. acknowledges partial support from NASA grant NAG5-1741, and S. D. acknowledges partial support from the NSF PYI award AST-9157412, J. M. M. and J. R. G. received partial support from NASA and NSF grants awarded to the California Institute of Technology.

REFERENCES

Aaronson, M., et al. 1982, ApJ, 258, 64
Arp, H. C. 1966, ApJS, 14, 1
Baade, W., & Minkowski, R. 1954, ApJ, 119, 215
Balick, B., & Heckman, T. 1979, AJ, 84, 302
Barthel, P. D. 1989, ApJ, 336, 606
Barvainis, R., Alloin, D., & Antonucci, R. 1989, ApJ, 337, L69
Baum, S. A., Heckman, T., Bridle, A., van Breugel, W., & Miley, G. 1988, ApJS, 68, 643
Bloemen, J. B. G. M., et al. 1986, A&A, 154, 25
Burbidge, G., & Crowne, A. H. 1979, ApJS, 40, 583
Bushouse, H. A., & Stanford, S. A. 1992, ApJS, 79, 213
Cataloged Galaxies and Quasars Detected in the *IRAS* Survey 1985, prepared by C. J. Persons, G. Helou, J. C. Good, & W. L. Rice (JPL D1932)
Colla, G., Fanti, C., Fanti, R., Gioia, I., Lari, C., Lequeux, J., Lucas, R., & Ulrich, M. H. 1975, A&AS, 20, 1
Condon, J. J., & Broderick, J. J. 1991, AJ, 102, 1663
Condon, J. J., Helou, G., Sanders, D. B., & Soifer, B. T. 1990, ApJS, 73, 359
Dickman, R. L., Snell, R. L., & Schloerb, F. P. 1986, ApJ, 309, 123
Djorgovski, S., Weir, N., Matthews, K., & Graham, J. R. 1991, ApJ, 372, L67
Draine, B. T., & Lee, H. M. 1984, ApJ, 285, 89
Faber, S. M., & Gallagher, J. S. 1976, ApJ, 204, 365
Fanaroff, B. L., & Riley, F. M. 1974, MNRAS, 167, 31P
Golombek, D., Miley, G. K., & Neugebauer, G. 1988, AJ, 95, 26
Heckman, T. M., et al. 1986, ApJ, 311, 525
Helou, G., Soifer, B. T., & Rowan-Robinson, M. 1985, ApJ, 298, L7
Impey, C. D., Wynn-Williams, C. G., & Becklin, E. E. 1990, ApJ, 356, 62
Kellerman, K. I., Sramek, R., Schmidt, M., Shaffer, D. B., & Green, R. 1989, AJ, 98, 1195
Knapp, G. R., Bies, W. E., & van Gorkom, J. H. 1990, AJ, 99, 476
Knapp, G. R., & Patten, B. M. 1991, AJ, 101, 1609
Lees, J. F., Knapp, G. R., Rupen, M. P., & Phillips, T. G. 1990, ApJ, 379, 177
MacKenty, J. W., & Stockton, A. 1984, ApJ, 283, 64
Mazzarella, J. M., Gaume, R. A., Soifer, B. T., Graham, J. R., Neugebauer, G., & Matthews, K. 1991, AJ, 102, 1241
Miller, J. S., & Goodrich, R. W. 1990, ApJ, 355, 456
Mirabel, I. F. 1989, ApJ, 340, L13
———. 1990, ApJ, 352, L37
Mirabel, I. F., & Sanders, D. B. 1988, ApJ, 335, 104
Mirabel, I. F., Sanders, D. B., & Kazes, I. 1989, ApJ, 340, L9
Moles, M., del Olmo, A., Masegosa, J., & Perea, J. D. 1988, A&A, 197, 1
Morganti, R., Ulrich, M.-H., & Tadhunter, C. N. 1992, MNRAS, 254, 546
Parma, P., Cameron, R. A., & de Ruiter, H. R. 1991, AJ, 102, 1960
Parma, P., de Ruiter, H. R., Fanti, C., & Fanti, R. 1986, A&AS, 64, 135
Phillips, T. G., Ellison, B. N., Keene, J. B., Leighton, R. B., Howard, R. J., Masson, C. R., Sanders, D. B., Veidt, B., & Young, L. 1987, ApJ, 322, L73
Radford, S. J. E., Solomon, P. M., & Downes, D. 1991, ApJ, 368, L15
Sanders, D. B., Scoville, N. Z., & Soifer, B. T. 1988, ApJ, 335, L1
———. 1991, ApJ, 370, 158
Sanders, D. B., Scoville, N. Z., Zenus, A., Soifer, B. T., Wilson, T. L., Zylka, R., & Steppe, H. 1989, A&A, 231, L5
Sanders, D. B., Soifer, B. T., Elias, J. H., Madore, B. F., Matthews, K., Neugebauer, G., & Scoville, N. Z. 1988a, ApJ, 325, 74
Sanders, D. B., Soifer, B. T., Elias, J. H., Neugebauer, G., & Matthews, K. 1988b, ApJ, 328, L35
Scoville, N. Z., & Good, J. C. 1989, ApJ, 339, 149
Scoville, N. Z., & Sanders, D. B. 1987, in Interstellar Processes, ed. H. Thronson & D. Hollenbach (Dordrecht: Reidel), 21
Scoville, N. Z., Sargent, A. I., Sanders, D. B., & Soifer, B. T. 1991, ApJ, 366, L5
Soifer, B. T., Boehmer, L., Neugebauer, G., & Sanders, D. B. 1989, AJ, 98, 766
Solomon, P. M., Rivolo, A. R., Barrett, J., & Yahil, A. 1987, ApJ, 319, 730
Tinney, C. G., Scoville, N. Z., Sanders, D. B., & Soifer, B. T. 1990, ApJ, 362, 473
van der Hulst, J. M., Golisch, W. F., & Haschick, A. D. 1983, ApJ, 264, L37
Vorontsov-Velyaminov, B. A. 1959, Atlas and Catalog of Interacting Galaxies (Moscow: Sternberg Inst.)
Walker, R. C., Benson, J. M., & Unwin, S. C. 1987, ApJ, 316, 546
Young, J. S., Schloerb, F. P., Kenney, J. D., & Lord, S. D. 1986, ApJ, 304, 443
Young, J. S., Xie, S., Kenney, J. D. P., & Rice, W. L. 1989, ApJS, 70, 699